TRANSVERSE OSCILLATIONS BEAMFORMER DESIGN FOR SECTOR SCAN USING BACK-PROPAGATION

Xinxin. GUO[1], D. Friboulet[1], H. Liebgott[2]
CREATIS, CNRS UMR 5220, INSERM U1044, Université de Lyon, INSA Lyon
[1] INSA Lyon, [2] Université Lyon 1
Lyon, France

Abstract— Echocardiographic acquisition based on point spread function (PSF) with transverse oscillations (TO) has been shown to be an efficient image formation technique for improving the accuracy of motion estimation in the transverse direction (direction perpendicular to the propagation axis). To date, beamforming yielding TO has mainly been developed for acquisitions performed in linear geometry. However, one of the most important applications of motion estimation is cardiac imaging, which implies acquisition done in sectorial geometry. In this framework, this paper describes a new beamformer design method as well as the corresponding implementation allowing for transverse oscillations for sector scan. The proposed method uses a back-propagation (BP) approach. The performance of this beamformer is quantitatively evaluated through numerical simulations. In particular, we show that the obtained PSF are closer to the expected ones as compared to PSF obtained using the conventional Fraunhofer approximation and the associated Fourier relation.

Keywords: beamforming, echocardiography, transverse oscillations, back-propagation

I. INTRODUCTION

It is of great importance to accurately image the motion of moving organs in clinical diagnosis. Echography is particularly well adapted for motion estimation (e.g., echocardiography, blood flow, elastography), due to its high frame-rate capacity. In cardiac imaging, conventional echocardiography is however facing some difficulties to estimate the motion of the heart with high accuracy in the transverse direction (the direction perpendicular to the beam axis). Working on the image formation, this problem can be addressed by modifying the beamforming scheme in order to introduce transverse oscillations (TO) in the system point spread function (PSF).

Transverse oscillations methods firstly arose in the 1990s in the field of blood flow estimation. Several groups have been working on these methods. Until now, TO methods have been applied in blood flow estimation by Jensen et al. [1] and Anderson [2], in elastography by Sumi [3, 4] and our group [5, 6], and in echocardiography based on different beamforming strategies and estimators.

These studies have shown that TO images can lead to improved 2D motion estimation in linear geometry. The formation of images featuring TO in linear geometry uses conventional beamforming designed using the Fraunhofer approximation, which allows relating the apodization function and the system PSF through a simple Fourier transform. Application of TO in echocardiography implies adapting this technique for sectorial scans. However, our preliminary investigations [7] have shown that conventional, Fraunhofer-based beamforming yields unsatisfactory TO patterns. Therefore in this paper we propose a new TO beamformer design for sector scan using back-propagation (BP).

The paper is organized as follows: in section II we briefly recall the principle of obtaining TO images in linear geometry using Fraunhofer approximation and give the transform from linear to sectorial geometry, the principle of BP and its application in sector scan; section III provides the evaluation of the accuracy of proposed BP method, and a comparison with conventional beamforming; section IV is the discussion and in section V we give the conclusion.

II. PRINCIPLE OF TRANSVERSE OSCILLATIONS AND BACK-PROPAGATION

The formation of TO images implies controlling the shape of the PSF. This control is obtained through a specific beamforming scheme, i.e. specific delay and apodization functions imposed to the different elements of the probe. In this section, we first recall how to design the beamformer parameters in order to obtain TO images using conventional Fraunhofer approximation and then we explain our proposed BP method.

A. Principle of Transverse Oscillations using Fraunhofer approximation

Fraunhofer approximation for linear geometry

In TO, we expect the lateral PSF profile to show the same kind of oscillations as those naturally present in the axial direction. In a linear geometry setting, such a lateral profile [8] can be expressed in eq. (1), where the expected profile is a multiplication of a Gaussian envelope with a cosine function. Here λ_x is the expected lateral wavelength, σ_x is the half maximum width of the Gaussian envelop, and $u_x = 1/\lambda_x$.

$$h(x) = \cos(2\pi u_x) \cdot \exp(-\pi(\frac{x}{\sigma_x})^2) \quad (1)$$

In order to obtain this kind of profile, we need to do specific beamforming. The classical beamformer design method is based on the Fraunhofer approximation, the conditions of which are met at the focal point. In order to be able to apply the Fraunhofer approximation along the whole propagation path, the delay function is set so as to perform dynamic quadratic focusing. Under this approximation, the transverse profile of the PSF at the depth of focusing is related to the apodization function by a Fourier transform[9]. As a consequence in order to obtain a TO PSF profile, the apodization function is taken as the inverse Fourier transform of (1), which is expressed as follows:

$$w_r(x) = \frac{1}{2}(\exp^{-\pi(\frac{x-x_0}{\sigma_0})^2} + \exp^{-\pi(\frac{x+x_0}{\sigma_0})^2}) \quad (2)$$

Where $x_0 = \lambda y/\lambda_x$ and $\sigma_0 = \sqrt{2}\,\lambda y/\sigma_x$, λ is the wavelength of the transmitted pulsed, y is the depth of interest, $\pm x_0$ is the position of the two peaks and σ_0 is half maximum width of each peak. The lateral PSF profile in eq. (1) and the apodization function (2) are represented in **Fig 1**.

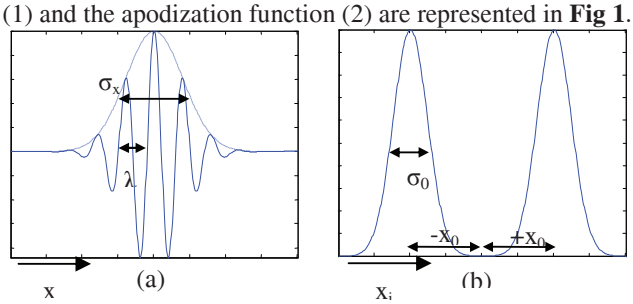


Figure 1: Representation of the lateral PSF profile (a) and the corresponding apodization function in (b).

Fraunhofer approximation for sectorial geometry

The above framework has been derived for linear geometry. Adapting it to sectorial geometry implies transforming the model parameters from Cartesian coordinates to polar coordinates. This is done by setting (see **Fig. 2**): $\lambda_x \approx \lambda_\theta \cdot r$, $\sigma_x = \sigma_\theta \cdot r$, and $y \approx r$, where λ_θ is the expected lateral wavelength of PSF profile in radians, σ_θ is the standard deviation of PSF profile, and r is the sweeping radius. Based on the approximation settings above, the position of two peaks $\pm x_{\theta 0}$ and the standard deviation $\sigma_{\theta 0}$ of the apodization function are given as follows:

$$x_{\theta 0} \approx \lambda/\lambda_\theta \quad (3)$$

$$\sigma_{\theta 0} \approx \sqrt{2}\lambda/\sigma_\theta \quad (4)$$

what's interesting in eq. (3)-(4) is that $x_{\theta 0}$ and $\sigma_{\theta 0}$ are no longer depend on depth like in linear geometry, but the lateral wavelength and the stand deviation of PSF profile.

B. Principle of Back-propagation

Back-propagation for linear geometry

TO images obtained using Fourier relation does not match well with expected profiles. This results from the Fraunhofer assumption, under which the Inverse Fourier Transform of PSF profile provides only an approximation of the apodization function. The limitation of Fraunhofer approximation drives us to propose a new TO beamformer design using BP which can provide more accurate images.

The PSF pressure field can be considered as a combined effect of ultrasound signals sent by all the aperture elements. For ultrasound signals, the Green function is used to model the propagation function from the ith element to a point of interest [9]. In a linear geometry setting, this case the pressure p(x,y) at the depth y and lateral position x is equal to

$$p(x,y) = \sum_{i=1}^{N} w(x_i) \frac{e^{\frac{j2\pi r_i}{\lambda}}}{r_i} \quad (5)$$

Where N is the number of active elements, x_i is the position of ith element, r_i is the distance from the ith element to the point of interest.

By using the reciprocity theorem, the apodization function in eq. (5) is equal to the pressure that would be observed at the aperture elements position of a probe located at the depth of interest and apodized with the expected pressure profile. This approach is thus called BP of the pressure field towards the aperture and can be expressed as

$$w_r(x_i, y_0) = \int_{-\infty}^{+\infty} p(x, y_0) \frac{e^{\frac{j2\pi r_{i0}}{\lambda}}}{r_{i0}} dx \quad (6)$$

Where y_0 is the depth of interest, $p(x, y_0)$ is the pressure profile at the depth of interest, r_{i0} is the distance between ith element and the point of interest.

Back-propagation for sectorial geometry

In linear geometry configuration, the expected PSF profile changes with lateral positions at the same depth, whereas for sector scan the profile changes with angles at the same scanning radius. **Fig.2** shows a sectorial geometry configuration.

Fig. 2(a) and **(b)** correspond to different situations when the beam sweeps in the direction θ_1 and θ_2 respectively. Θ is the angle of scan area, r_0 is the scan radius. Apodization functions which are presented as $w_{r1}(x, r_0)$ and $w_{r2}(x, r_0)$ corresponding to expected profiles of $p(\theta_1, r_0)$ and $p(\theta_2, r_0)$ respectively.

Based on **Fig. 2**, the basic idea of BP could be explained as follows: the scanner sends a beam sweeping the area of interest. For each direction, at the different point of interest, we expect the same shape of PSF profile. Therefore, according to the same shape of PSF profile, we can calculate the apodization function that should be imposed to aperture. From eq. (6), the apodization function adapted to sectorial geometry can be expressed as in eq. (7).

$$w_r(x_i, r_0) = \int_{-\frac{\Theta}{2}}^{\frac{\Theta}{2}} p(\theta, r_0) \frac{e^{\frac{j2\pi r_{i0}}{\lambda}}}{r_{i0}} d\theta \qquad (7)$$

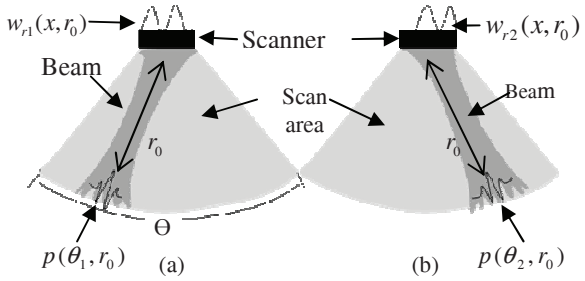


Figure 2: Presentation of sector scan using back-propagation with transverse oscillations. Θ is the angle of scan area, θ_1 and θ_2 are the different scan directions, r_0 is the scan radius. Apodization functions which are presented as $w_{r1}(x, r_0)$ and $w_{r2}(x, r_0)$ corresponding to expected profiles of $p(\theta_1, r_0)$ and $p(\theta_2, r_0)$ respectively.

III. SIMULATIONS AND RESULTS

Numerical simulations are performed using the software Field II[10, 11]. The number of active elements is equal to 64. The dimension of elements is 5mm×λ/2 (height × width), λ is the ultrasound wave length. The distance between two elements is 0.1mm. Center frequency of transmit signals is 3MHz, and sampling frequency is 100MHz.

The accuracy is evaluated by comparing the expected, theoretical point spread function PSF^{th}, and the PSF resulting from the simulation by applying a beamforming/ apodization scheme, PSF^{exp}. In these experiments we applied either the proposed BP approach or the conventional Fourier based technique. The accuracy is quantified using the root mean square error (RMSE) as defined below. Calling PSF_i^{th} the i^{th} value of the theoretical expected PSF and PSF_i^{exp} the PSF using Fourier relation or BP, the RMSE is given as in eq.(8). PSF images are obtained with the scatters located in the front and on the side of aperture as well as at different depth. We pay specific attentation on the side of the sector as it corresponds to the place where the most important error will be observed. At the same time, it

$$RMSE = \sqrt{\frac{1}{N}\sum_{i}^{N}(PSF_i^{th} - PSF_i^{\exp})^2} \qquad (8)$$

is also a test of the adaptive performance of our method.

The images of apodization functions in sector scan are shown in Figure 3. Parameters are set as $\lambda_\theta = 4°$ and $\sigma_\theta = 1.5\lambda_\theta$.

Fig. 3 presents the apodization function for sector scan. **Fig. 3(a)** give a comparison of apodization function obtained using Fourier relation and BP in the direction of 0°. Furthermore, **Fig. 3(b)** presents the apodization obtained in different angles using BP and **(c)** is the presentation of apodization functions corresponding to directions 30 and -30°, as indicated in **Fig. 3(b)**.

Fig. 3(b) shows that the apodization function is asymmetric with respect to the central element. This can be better seen from **Fig. 3(c)** which shows the apodization profile for directions -30° and 30°.

A comparison of expected PSF profiles obtained using Fourier relation and the proposed BP method is presented in **Fig. 4** for different depths and different directions.

IV. DISCUSSION

Fig. 4(a) shows the PSF profiles obtained in the direction of 0° and a depth of 60 mm. It may be observed that the profiles corresponding to BP are slightly closer to the expected ones as compared to the profiles associated to Fourier-based beamforming. This is confirmed by the RMSE which is equal to $3.86\text{x}10^{-2}$ for the Fourier-based profiles and which is $3.04\text{x}10^{-2}$ for the BP-based profiles in **Fig. 4(a)**, which indicates that BP-based method brings an improvement of 21%. Profiles obtained in the same direction than (a) but with a depth are of 70 mm presented in **Fig 4(b)** and yields the same conclusion: the profile associated to BP leads the same accuracy than the Fourier-based profile, with a RMSE equal to $3.62\text{x}10^{-2}$ for BP and $4.26\text{x}10^{-2}$ for Fourier-based beamforming, which also brings an improvement of 15% when compare with the Fourier-based profile. Here the improvement is smaller as radian changes slightly at larger depth, thus the approximation expressed in eq. (3)-(4) brings little and little error with deeper depth when using Fraunhofer approximation. It changes when observing the results obtained for direction far from the probe axis. shows the results obtained for a

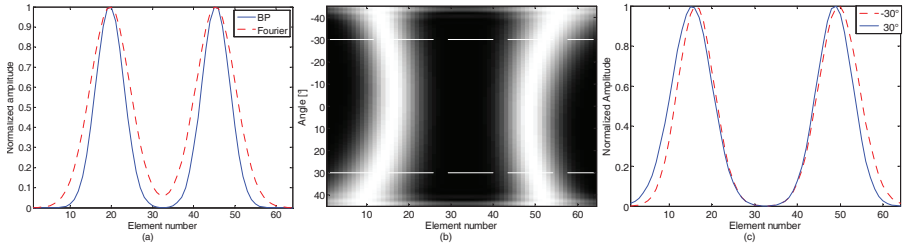


Figure 3:Presentation of apodization functions for sector scan: (a) presents apodized profiles using Fourier relation in dotted line and back-propagation in solid line in 0°; (b) is apodization function of BP for all sweeping angles; (c) gives the indicated apodization for directions 30 and -30°, corresponding to the two dotted lines in (b).

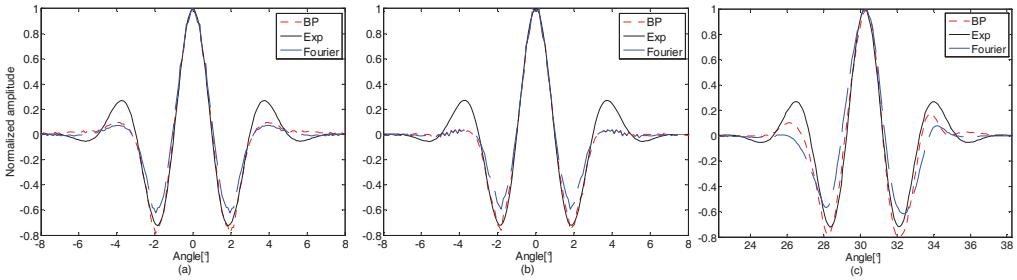


Figure 4: PSF profiles obtained in direction of 0° at different depth: 60 mm in (a) and 70 mm in (b). (c) presents the PSF profiles obtained in the direction of 30° at the depth of 60 mm. The profiles in dotted lines are obtained using Fourier relation, BP in dashed lines and expected profiles in solid lines.

direction of 30° away from this axis. **Fig. 4(c)** shows the improvement brought by BP over Fourier-based beamforming, which is confirmed by the RMSE which is equal to 6.46 $x10^{-2}$ for the Fourier-based profile and 3.59 $x10^{-2}$ for the BP-based, not difficult to see that our proposed method brings almost an improvement of 50%.

The difference between obtained profiles and expected PSFs is resulting from several aspects: the approximate transformation from x_0 and σ_0 in Cartesian coordinates to $x_{\theta 0}$ and $\sigma_{\theta 0}$ in polar coordinates, which can be seen at the end of section II part A;the dimension of element is not negligible, yielding approximation error when the distance from the element to the point of interest is calculated; another factor is that the Green function used as the propagation function in eq. (5) is monochromatic whereas ultrasound image is obtained using broadband signals.

As in the case of the Fraunhofer approximation, using the proposed BP method the apodization function keeps also constant even if the depth changes in sector scan, as shown by eq. (3)-(4). As in simulations, the same apodization function can be imposed to all signals received in same direction, this can obviously reduce time cost.

Furthermore in order to improve the estimation accuracy one might be interested in decreasing the value of the lateral PSF wavelength. This would need larger probes, which is unfortunately not possible due to the acquisition that has to be done between the ribs for echocardiography. The quality of the estimation result might be improved with larger probes performing a sectorial scan for other medical applications.

V. CONCLUSION

In this paper, our methodology of transverse oscillation beamformer design using back-propagation has been introduced.

The improvement of our method has been observed when compared to Fourier relation. Further confirmation need to be done by using experimental acquisitions. The potential for diagnosing diseases can be evaluated in further studies.

VI. REFERENCES

[1] J. A. Jensen and P. Munk, "A new method for estimation of velocity vectors," *Ultrasonics, Ferroelectrics and Frequency Control, IEEE Transactions on,* vol. 45, pp. 837-851, 1998.

[2] M. E. Aderson, "Multi-dimensional velocity estimation with ultrasound using spatial quadrature," *Ultrasonics, Ferroelectrics and Frequency Control, IEEE Transactions on,* vol. 45, pp. 852-861, 1998.

[3] C. Sumi, "Multidimensional displacement vector measurement methods utilizing instantaneous phase," 2005, pp. 1704-1707.

[4] C. Sumi, "Displacement vector measurement using instantaneous ultrasound signal phase-multidimensional autocorrelation and Doppler methods," *Ultrasonics, Ferroelectrics and Frequency Control, IEEE Transactions on,* vol. 55, pp. 24-43, 2008.

[5] H. Liebgott, J. Fromageau, J. E. Wilhjelm, D. Vray, and P. Delachartre, "Beamforming scheme for 2D displacement estimation in ultrasound imaging," *EURASIP journal on applied signal processing,* vol. 2005, pp. 1212-1220, 2005.

[6] H. Liebgott, J. E. Wilhjehm, J. A. Jensen, D. Vray, and P. Delachartre, "PSF dedicated to estimation of displacement vectors for tissue elasticity imaging with ultrasound," *Ultrasonics, Ferroelectrics and Frequency Control, IEEE Transactions on,* vol. 54, pp. 746-756, 2007.

[7] H. Liebgott, A. Basarab, S. Marincas, O. Bernard, and D. Friboulet, "Tangential oscillations for motion estimation in echocardiography," 2008, pp. 1761-1764.

[8] H. Liebgott, "Impulse response synthesis in ultrasound imaging for vectorial displacement estimation", Ph.D. thesis, 2005.

[9] J. W. Goodman, *Introduction to Fourier optics*: Roberts & Company Publishers, 2005.

[10] J. A. Jensen and N. B. Svendsen, "Calculation of pressure fields from arbitrarily shaped, apodized, and excited ultrasound transducers," *Ultrasonics, Ferroelectrics and Frequency Control, IEEE Transactions on,* vol. 39, pp. 262-267, 1992.

[11] J. A. Jensen, "Field: A program for simulating ultrasound systems," 1996.